EURASIP Journal on Wireless Communications and Networking 2004:1, 32–45

CDMA Downlink Transmission with Transmit Antenna Arrays and Power Control in Multipath Fading Channels

Huaiyu Dai
Department of Electrical and Computer Engineering, NC State University, Raleigh, NC 27695-7511, USA
Email: huaiyu_dai@ncsu.edu

Laurence Mailaender
Wireless Communications Research Department, Bell Labs, Lucent Technologies, Holmdel, NJ 07733, USA
Email: lm@lucent.com

H. Vincent Poor
Department of Electrical Engineering, Princeton University, Princeton, NJ 08544, USA
Email: poor@princeton.edu

Received 20 August 2003; Revised 11 March 2004

Wireless code-division multiple-access (CDMA) cellular downlink communications with transmit antenna arrays in multipath fading channels is studied. Various array signal processing techniques at the transmit end are investigated and compared under various settings, in conjunction with power control. No instant downlink channel information is assumed; however, the obtained results are also compared with results assuming ideal feedback. The study is carried out for both circuit-switched and packet-switched systems, where different goals are pursued and different conclusions are drawn. In particular, it is found that the traffic type impacts the algorithm choice in downlink transmission, and that there is no need to seek optimum power control/allocation schemes, which are either too complex or infeasible in practice. Another interesting conclusion is that, even though feedback does not help much for packet-switched systems, it does help for circuit-switched systems, the gain of which increases with the number of antennas.

Keywords and phrases: CDMA, downlink transmission, multipath fading, power control, transmit arrays.

1. INTRODUCTION

Cellular base stations may make use of an antenna array to achieve diversity gains or antenna gains so as to improve the system capacity. In a fading environment, the antenna elements should be separated sufficiently far apart to experience uncorrelated fading and to thereby achieve the diversity gain [1]. In urban areas, the required spacing is half a wavelength at the mobile and ten times a wavelength at the base station. Independent of the fading environment and in addition to the diversity gain, multiple antennas can provide antenna gain due to the potential coherent combining of the transmitted and/or received signals and the underlying uncorrelated noise. This technique is usually called beamforming, where the signals are modeled as planar wavefronts impinging on/transmitted from an antenna array with a certain direction of arrival (DOA)/direction of departure (DOD) [2]. In the beamforming approach, the antenna elements are usually closely spaced so that correlated fading coefficients are obtained for the elements of an antenna array, which form a vector called the spatial signature or the steering vector. The spatial signature, analogous to the spreading signature in the direct-sequence code-division multiple-access (DS-CDMA) systems, is often exploited for interference suppression. In this study, we focus on array processing techniques to improve the CDMA cellular downlink transmission, which is foreseen to be of crucial importance for the next generation communication systems supporting wireless Internet, video on demand, and multimedia services. In particular, we will determine the optimal transmission schemes for both voice and data applications, and investigate the influence of the feedback and number of antennas.

Perhaps the simplest form of spatial processing is open loop transmit diversity, which will serve as the performance baseline in this study. Sectorization, which can be interpreted as fixed beam transmission, is well known to be an effective

way to improve the system capacity [3]. Other array processing techniques discussed in this paper belong to the beamforming category. A simple form of transmit beamforming is beam steering, which assumes knowledge of the mobile's position and forms a beam in the direction of line of sight (LOS). The performance of beam steering degrades in multipath channels with angle spread. A more sophisticated use of the array is to determine the antenna-weighting vector that maximizes signal-to-noise ratio (SNR) at the mobiles. Alternatively, one can borrow the idea from uplink receive array processing and come up with a maximum signal-to-interference ratio (SIR) solution for weighting vector design, that is, maximizing the ratio of the received power of the signal at the desired user and that leaked to the other users. Note that the downlink communication scenario is different from that of the uplink. While in the uplink the weighting vector designs for different users are decoupled, optimal beamforming for the downlink will have to be considered jointly, because the weighting vector for one user will impact the interference received by other users as well as the useful signal power received by the desired user. A joint power control and downlink beamforming algorithm has been proposed in [4, 5] according to some optimality criterion, and will also be used as the performance baseline.

Power control was conceived originally as a mechanism to deal with the near-far problem, but a more general emerging view is that it is a flexible mechanism to provide different quality of service to users with heterogeneous requirements [6]. For downlink transmission, power control is also important for energy conservation and interference mitigation. In circuit-switched systems, when we perform the above downlink transmission array processing together with power control, we execute it in two steps: (1) an array weighting vector is determined (not needed for transmit diversity) and the signal-to-interference-and-noise ratio (SINR) is calculated (as functions of transmitted powers) for each mobile receiver; (2) transmitted power is allocated among users so as to minimize the total transmitted power from the base station while keeping the SINRs of all links above a certain threshold. When there is no feasible solution for power allocation or the total transmitted power needed exceeds the maximum threshold, an outage is declared. The figure of merit for circuit-switched systems is the (simultaneously) supportable user capacity with certain SINR requirement under some outage limit. However, in packet-switched systems (such as HDR or HSDPA), where users are delay tolerant, we carry out rate control instead of power control, assuming the base station transmits at its maximum power. We mainly assume the powers are equally allocated among active users; but an optimal power allocation (OPA) scheme will also be studied. The figure of merit for the packet-switched systems is the total throughput (data rate), which is directly related to the SINR seen at the mobile users. Throughout this paper, no instant downlink channel state information (CSI) is assumed; however, the obtained results are also compared with results assuming ideal CSI. Both systems have a total transmitted power constraint.

This paper is organized as follows. In Section 2 the system model is introduced. Power control/allocation algorithms for circuit/packet-switched systems are addressed in Section 3 under a common framework. In Section 4, various transmit array processing techniques are presented, in conjunction with power control. Section 5 provides numerical comparison results for these array processing techniques under various settings for both circuit-switched and packet-switched systems. Section 6 concludes the paper.

2. SYSTEM MODEL

2.1. Multipath channel

We assume a CDMA frequency division duplex (FDD) cellular system. In each cell, K mobile users, each employing a single antenna, communicate with a base station having an M-element antenna array. The spreading codes employed within a cell by different users, or different antenna elements and different users (for code transmit diversity), are assumed to be mutually orthogonal with spreading gain N; while any two codes (either identical or different) with different delays (for different paths) are assumed to be independent. The physical channel between the mobile users and the base station is assumed to be wide sense stationary with uncorrelated scattering (WSSUS) multipath frequency-selective fading. We assume for simplicity that there are L paths for each user.

For the beamforming techniques, after joint transmission of the weighted signals bound for different users from the base station, the baseband signal received by the ith mobile user is given by

$$r_i(t) = \sqrt{G_i} \sum_{k=1}^{K} \sqrt{P_k} b_k \mathbf{w}_k^H \sum_{l=1}^{L} \alpha_{il}^D(t) \mathbf{a}^D(\theta_{il}) c_k(t - \tau_{il}) + n_i(t), \tag{1}$$

where P_k is the power assigned to the user k; b_k is the transmitted data for user k; $\mathbf{w}_k$ is the transmit beamforming weight vector for user k; $c_k(t)$ is the spreading waveform assigned to user k; G_i is the path gain from the transmit array to the ith user, which combines the effects of path loss and shadowing; τ_{il} is the delay of the lth path from the base-station antenna array to the ith user; $\alpha_{il}^D(t)$ describes the small-scale fading random process of the lth path from the base-station antenna array to the ith user, which is frequency dependent and largely uncorrelated for uplink and downlink; and θ_{il} is the angle of departure of the lth path from the base-station antenna array to the ith user. In our model, we assume that θ_{il}, $1 \le l \le L$, has a Gaussian distribution centered at $\theta_{i,\mathrm{LOS}}$, the LOS direction from the base-station antenna array to the ith user. With the assumptions of planar waves and a uniform linear array, the frequency-dependent downlink steering vector is given by

$$\mathbf{a}^D(\theta_{il}) = \left[1, e^{-j2\pi d_a (f_D/c)\sin(\theta_{il})}, \ldots, e^{-j2\pi d_a (M-1)(f_D/c)\sin(\theta_{il})}\right]^T, \tag{2}$$

where d_a is the interelement spacing of the antenna array and f_D is the downlink carrier frequency. Finally, $n_i(t)$ is the noise term, which includes the thermal background noise and the out-of-cell interference, to be further addressed in the sequel. In this paper, we are mainly interested in a chip-matched-filtered and chip-sampled discretized model, easily derived from (1) as

$$\mathbf{r}_i = \sqrt{G_i} \sum_{k=1}^{K} \sqrt{P_k} b_k \mathbf{w}_k^H \sum_{l=1}^{L} \alpha_{il}^D \mathbf{a}_{il}^D \mathbf{c}_k^{il} + \mathbf{n}_i, \tag{3}$$

where the length of the received vector is large enough to catch the signals from all L paths. We assume that the path delay is negligible compared to the spreading length, so that intersymbol interference (ISI) can be ignored.

While the base-station antenna elements should be closely spaced for beamforming techniques to get coherent signals across the antenna array, they should be widely separated to get diversity gain for transmit diversity schemes. Rather than being combined with a steering vector, the signals coming from different elements of an antenna array exploiting transmit diversity experience uncorrelated fading. Assuming a simple code transmit diversity scheme without code reuse,[1] the transmitted signal from the mth antenna can be modeled as

$$s_m(t) = \frac{1}{\sqrt{M}} \sum_{k=1}^{K} \sqrt{P_k} b_k c_{km}(t), \tag{4}$$

where $c_{km}(t)$ is the spreading code for the kth user in the mth antenna, and the total transmitted energy of one user is normalized with the number of transmit antennas. Note that while beamforming techniques applies different weights for each antenna element on the signals of one user, (code) transmit diversity assigns different spreading codes for each antenna element to the signals of one user. For the transmit diversity technique, the received signal at the ith mobile is given by

$$r_i(t) = \sqrt{\frac{G_i}{M}} \sum_{m=1}^{M} \sum_{k=1}^{K} \sqrt{P_k} b_k \sum_{l=1}^{L} \alpha_{ml}^i c_{km}(t - \tau_{il}) + n_i(t), \tag{5}$$

where it is noted that for each path of the multipath channels between each antenna element and the mobile user, even though the delays are not significantly different across the array, the instantaneous fading coefficients $\{\alpha_{ml}^i\}$ are uncorrelated. The other elements of (5) are self-explanatory. Again, it is preferable to deal with the discretized model given as

$$\mathbf{r}_i = \sqrt{\frac{G_i}{M}} \sum_{m=1}^{M} \sum_{k=1}^{K} \sqrt{P_k} b_k \mathbf{C}_{km}^i \mathbf{h}_m^i + \mathbf{n}_i, \tag{6}$$

where $\mathbf{C}_{km}^i = [\mathbf{c}_{km}^{i1}, \ldots, \mathbf{c}_{km}^{iL}]$, whose columns are discretized delayed versions of $c_{km}(t)$ corresponding to different paths, and $\mathbf{h}_m^i = [\alpha_{m1}^i, \ldots, \alpha_{mL}^i]^T$ collects the instantaneous small-scale fading coefficients of the L paths from the mth antenna to the ith user.

2.2. FDD framework

In FDD systems, the separation between the uplink and downlink carrier frequencies is large enough to reject the reciprocity principle. However, if the frequency separation is not too large, the uplink and downlink will still share many common features, among which are the number of radio paths, their delays and angles, the large-scale path loss and shadowing, and the variance of small-scale fading [8, 9]. Nevertheless, the instantaneous small-scale fading of the two links is uncorrelated, which makes the downlink problem more difficult for FDD systems. The signal received at the base station provides a means for directly estimating the uplink, not the downlink channel. While such information could be available via a feedback channel from the mobile, we assume that no such channel exists. The fact that the array response is also frequency dependent further complicates the problem.

Although the small-scale fading is uncorrelated between the uplink and downlink, their average strength is assumed to be insensitive to small changes in frequency [9, 10], that is,

$$E\left\{ \left| \alpha_{kl}^D \right|^2 \right\} = E\left\{ \left| \alpha_{kl}^U \right|^2 \right\}, \tag{7}$$

where the superscripts "D" and "U" denote downlink and uplink, respectively. Therefore, the long-term statistics of the downlink small-scale fading can be estimated via time average from uplink data. To estimate the downlink steering vectors, several approaches exist. One idea (the matched array) is to design two separate closely located arrays which are scaled versions of each other in proportion to the ratio of the uplink and downlink wavelengths, thus making the uplink and downlink steering vectors the same [9]. The drawbacks of this approach are cost, imperfect array matching, and near-field uneven scattering. A clever log-periodic array configuration is proposed in [10], which overlaps the two subarrays of M elements mentioned above into one $M+1$ array with $d_m/d_{m-1} = \lambda_U/\lambda_D$, where d_m is the spacing between the mth and the $(m+1)$th element. The drawbacks above are alleviated but still exist. Another approach (the duplex array) is to use a single array for both the uplink and downlink, and to transpose the array response from the uplink to the downlink via a linear transformation. However, some constraints are imposed to make the linear transformation tractable, for example, a small frequency shift assumption in [9] and circular array geometry in [11]. In our work, we exploit the approach of estimating the DODs from the uplink data through high-resolution DOA estimation methods or training sequences, assuming reciprocity principle holds for DODs and DOAs. We also ignore the estimation errors, which deserves further study. Then the downlink steering

[1] A total of KM Walsh codes are required. To conserve codes, techniques such as space-time spreading [7] can be used, but the performance achieved is not different.

vector is calculated through (2). In the sequel, the superscript "D" will be omitted for the beamforming model (3) when no ambiguity is incurred.

Throughout this paper, we assume that the downlink channel is known at the receiver, but only approximated at the transmitter.

2.3. Cellular system

We consider a cellular geometry as shown in Figure 1. It consists of two tiers of surrounding cells around the cell of interest. Each cell is divided into three sectors of 120 degrees unless otherwise indicated. Because CDMA is explored, mobile users in the sector of interest will suffer interference from adjacent sectors of the same cell, as well as from surrounding cells, as indicated in Figure 1. For simplicity, the out-of-cell/sector interference is assumed to be white and Gaussian and is included in the noise term of the model, so that only its power matters. Throughout this paper, we assume that the noise vector seen at mobile i is complex Gaussian with independent and identically distributed (i.i.d.) components of zero mean and variance σ_i^2. We assume that all cells and sectors are identical, which are loaded with the same number of users exhibiting the same behavior, and at the base stations the same operations are exploited. This model should reflect the average performance of actual systems in the long run.

3. POWER CONTROL/ALLOCATION ALGORITHMS

In different application scenarios, optimal power control/allocation may have different meanings. For a circuit-switched system, a commonly used criterion is formulated as follows:

$$\min \sum_{k=1}^{K} P_k \quad \text{s.t. } \text{SINR}_k \geq \gamma_k,\ 1 \leq k \leq K, \tag{8}$$

that is, minimize the total transmitted power with the constraints that each link attains an SINR above a certain threshold. For a packet-switched system, we always transmit at the maximum power, and we are concerned with the throughput of the network. We can simply allocate power equally among the active users, or we can allocate power in some optimal way. An optimal power assignment scheme proposed in [12] is formulated as follows:

$$\max \text{SINR}_{\min} \quad \text{s.t. } \sum_{k=1}^{K} P_k \leq P_{\max}, \tag{9}$$

that is, maximize the minimum link SINR with the total transmitted power constraint. This scheme tries to be fair to all users, which is not necessarily a good strategy for maximal throughput without taking into consideration the data link budget and network schedule.

It turns out that these two power control/allocation schemes are related to the same algebraic theorem given as follows [13].

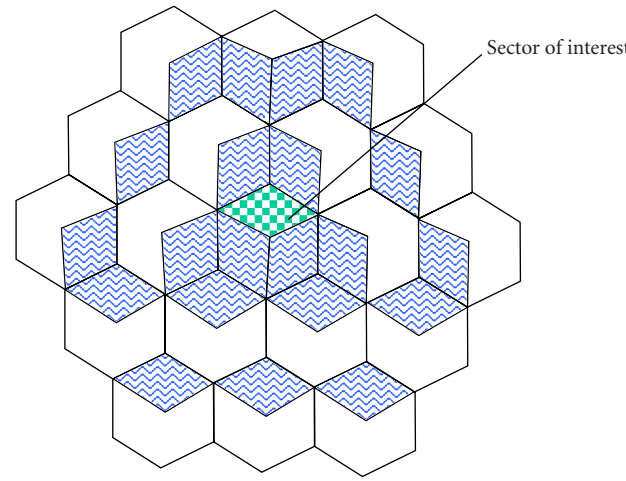

Figure 1: Cellular simulation model.

3.1. Perron-Frobenius theorem and its applications

Theorem 1. *Suppose* $\mathbf{T}$ *is an* $n \times n$ *nonnegative*[2] *irreducible matrix. Then there exists an eigenvalue* r *such that*

(a) r *is real and positive;*
(b) r *is associated with strictly positive left and right eigenvectors;*
(c) $r = \max\{|\lambda_i|\} = \rho(\mathbf{T})$, *where* λ_i, $1 \leq i \leq n$, *are the eigenvalues of the matrix* $\mathbf{T}$, *and* $\rho(\mathbf{T})$ *denotes its spectral radius;*
(d) r *has algebraic multiplicity 1;*
(e) $\min_i \sum_{j=1}^{n} t_{ij} \leq r \leq \max_i \sum_{j=1}^{n} t_{ij}$ *with equality on either side implying equality throughout. A similar result holds for column sums.*

Application 1. A necessary and sufficient condition for a nonnegative (nontrivial[3]) solution $\mathbf{x}$ to the equations $(s\mathbf{I} - \mathbf{T})\mathbf{x} = \mathbf{c}$ to exist for any nonnegative (nontrivial) vector $\mathbf{c}$ is that $s > r$. In this case there is only one strictly positive solution given by $(s\mathbf{I} - \mathbf{T})^{-1}\mathbf{c}$.

Application 2. If a nonnegative (nontrivial) vector $\mathbf{y}$ satisfies $\mathbf{T}\mathbf{y} \leq s\mathbf{y}$ $(s > 0)$, then $\mathbf{y} > 0$, $s \geq r$, and $s = r$ if and only if $\mathbf{T}\mathbf{y} = s\mathbf{y}$.

3.2. General form of power-control/allocation solutions

The power-control criterion of (8) is related to Application 1 of the theorem as follows. The general form of the power-control problem can be reformulated as

$$\min \sum_{k=1}^{K} P_k \quad \text{s.t. } (\mathbf{I} - \mathbf{DF})\mathbf{p} = \mathbf{u}, \tag{10}$$

[2] Here the term nonnegative refers to a vector or matrix all of whose elements are nonnegative. The definition for strictly positive is similar.

[3] A trivial vector or matrix is one having all-zero elements.

where $\mathbf{I}$ is a K by K identity matrix, $\mathbf{D}$ is a diagonal matrix with entries $\gamma_1, \ldots, \gamma_K$, $\mathbf{F}$ is a nonnegative irreducible matrix (interference term), $\mathbf{p} = [P_1, P_2, \ldots, P_K]^T$ collects the powers assigned to all users, and $\mathbf{u}$ is a positive vector (noise term).[4] So we have a feasible (nonnegative) solution for the power allocation vector if and only if the spectral radius of $\mathbf{DF}$ is less than one, otherwise we will claim an outage occurs. We call this a type-I outage and call the case in which we do get a nonnegative solution but the total transmitted power exceeds the maximum threshold, that is, $\mathbf{p}^T\mathbf{1} > P_{\max}$, a type-II outage. The solution to (10), if it exists, is given by $(\mathbf{I} - \mathbf{DF})^{-1}\mathbf{u}$ or alternatively by Jacobi iteration

$$\mathbf{p}^{(n+1)} = \mathbf{u} + \mathbf{DF}\mathbf{p}^{(n)}, \tag{11}$$

which will converge for any initial value in this setting.

The power allocation criterion of (9) is related to Application 2 of the theorem as follows. It can easily be shown that this optimization scheme results in equal SINR $= \gamma$ for all links. The objective functions then become

$$\mathbf{p} = \gamma(\mathbf{F}\mathbf{p} + \mathbf{h}), \qquad \mathbf{p}^T \cdot 1 = P_{\max}, \tag{12}$$

with $h_i = u_i/\gamma$. On writing $\mathbf{y} = [\mathbf{p}^T, 1]^T$, we can rewrite (12) as

$$\mathbf{T}\mathbf{y} = \gamma\mathbf{Q}\mathbf{y} \tag{13}$$

with

$$\mathbf{T} = \begin{bmatrix} \mathbf{I}_{K\times K} & \mathbf{0}_{K\times 1} \\ \mathbf{1}^T & -P_{\max} \end{bmatrix}, \qquad \mathbf{Q} = \begin{bmatrix} \mathbf{F} & \mathbf{h} \\ \mathbf{0}_{1\times K} & 0 \end{bmatrix}, \tag{14}$$

where $\mathbf{1}$ is an all-1 vector. Alternatively, we can write it as

$$\mathbf{R}\mathbf{y} = \frac{1}{\gamma}\mathbf{y}, \tag{15}$$

with

$$\mathbf{R} = \mathbf{T}^{-1}\mathbf{Q} = \begin{bmatrix} \mathbf{F} & \mathbf{h} \\ \dfrac{\mathbf{1}^T\mathbf{F}}{P_{\max}} & \dfrac{\mathbf{1}^T\mathbf{h}}{P_{\max}} \end{bmatrix}. \tag{16}$$

It is easily shown that $\mathbf{R}$ is a nonnegative irreducible matrix. So we always have a unique positive solution for $\mathbf{p}$ and the SINR margin is the reciprocal of the largest eigenvalue of $\mathbf{R}$.

4. ARRAY SIGNAL PROCESSING

In this section, various array signal processing techniques are discussed in detail, among which are transmit diversity, sectorization, and beamforming techniques including beam steering, maximum SNR beamforming, and maximum SIR or SINR beamforming. We assume that the mobile receiver can learn the fading channel and perform RAKE combining. So the instantaneous SINR is obtained for each scheme, based on which the power control of Section 3 is then applied. A joint power control and beamforming algorithm [5] is also discussed, and its optimality is verified in our setting.

4.1. Transmit diversity

We exploit code transmit diversity for downlink CDMA communications. The data streams of all users are transmitted simultaneously. For each user each data symbol is transmitted with equal power from every antenna using multiple mutually orthogonal spreading codes. On denoting $\mathbf{b} = [b_1, \ldots, b_K]^T$, $\tilde{\mathbf{l}}^i_{km} = \mathbf{C}^i_{km}\mathbf{h}^i_m$, $\mathbf{l}^i_k = \sum_{m=1}^{M} \tilde{\mathbf{l}}^i_{km}$, $\mathbf{L}^i = [\mathbf{l}^i_1, \ldots, \mathbf{l}^i_K]$, and $\mathbf{P} = \sqrt{G_i/M}\,\mathrm{diag}(\sqrt{P_1}, \ldots, \sqrt{P_K})$, (6) can be rewritten as

$$\mathbf{r}_i = \mathbf{L}^i\mathbf{P}\mathbf{b} + \mathbf{n}_i. \tag{17}$$

A standard space-time RAKE receiver yields

$$\begin{aligned}(\mathbf{l}^i_i)^H\mathbf{r}_i = {} & \sqrt{\frac{G_i}{M}}\sqrt{P_i}\left\{(\mathbf{l}^i_i)^H\mathbf{l}^i_i\right\}b_i \\ & + \sum_{k\neq i}\sqrt{\frac{G_i}{M}}\sqrt{P_k}\left\{(\mathbf{l}^i_i)^H\mathbf{l}^i_k\right\}b_k + \left\{(\mathbf{l}^i_i)^H\mathbf{n}_i\right\}.\end{aligned} \tag{18}$$

Assuming that

$$\left\langle \mathbf{c}^{i,l1}_{k1,m1}, \mathbf{c}^{i,l2}_{k2,m2} \right\rangle = \begin{cases} 1, & l1 = l2,\ k1 = k2,\ m1 = m2, \\ 0, & l1 = l2,\ (k1, m1) \neq (k2, m2), \\ \beta, & l1 \neq l2, \end{cases} \tag{19}$$

where β is a random variable with

$$E\{\beta\} = 0, \qquad E\{\beta^2\} = \frac{1}{N}, \tag{20}$$

and on denoting

$$\begin{aligned} A^i &= \sum_{m=1}^{M}\sum_{l=1}^{L}|\alpha^i_{ml}|^2, \\ C^i &= \frac{1}{N}\sum_{m}\sum_{m'}\sum_{l}\sum_{l'\neq l}|\alpha^i_{ml}|^2|\alpha^i_{m'l'}|^2, \end{aligned} \tag{21}$$

the SINR for user i is given by[5]

$$\begin{aligned}&\mathrm{SINR}_i \\ &= \frac{\dfrac{G_i}{M}P_i\left[(A^i)^2 + \dfrac{4}{N}\sum_{m}\sum_{l}\sum_{m'}\sum_{l'\neq l}{}_{(m'-1)L+l'>(m-1)L+l}\mathrm{Re}(\alpha^i_{ml}\alpha^i_{m'l'})^2\right]}{\sum_{k\neq i}\dfrac{G_i}{M}P_kC^i + \sigma_i^2A^i} \\ &\approx \frac{\dfrac{G_i}{M}P_i(A^i)^2}{\sum_{k\neq i}\dfrac{G_i}{M}P_kC^i + \sigma_i^2A^i}.\end{aligned} \tag{22}$$

[4] Exact SINR formulas will be given in the next section, together with the definitions for $\mathbf{F}$ and $\mathbf{u}$.

[5] The cross-correlation terms can typically be discarded due to their insignificance (attenuated by a factor of spreading gain).

The power-control formula (10) is exemplified here with

$$\mathbf{D} = \operatorname{diag}(\gamma_1, \ldots, \gamma_K),$$
$$F_{ij} = \begin{cases} 0, & i = j, \\ \dfrac{C^i}{(A^i)^2}, & i \neq j, \end{cases} \qquad u_i = \frac{\gamma_i \sigma_i^2 M}{G_i A^i}. \tag{23}$$

4.2. Sectorization

The cochannel interference in a cellular system may be decreased by replacing omnidirectional antennas with directional antennas, each radiating within a specified sector. Sectorization usually increases users' SINR or equivalently increases the system capacity, at the expense of increased numbers of antennas and decrease in trunking efficiency. The sectorizing antenna radiation pattern adopted in this paper is formulated as follows:

$$G_S(\theta) = \begin{cases} 1 - \dfrac{(1-b)}{(\pi/S)^2}\theta^2, & |\theta| \leq \sqrt{\dfrac{1-a}{1-b}}\dfrac{\pi}{S}, \\ a, & \text{elsewhere}, \end{cases} \tag{24}$$

where $G_S(\theta)$ is the gain of the antenna in a direction at angle θ relative to the maximal gain direction, a denotes the front-to-back ratio, b denotes the attenuation at sector crossover, and S is the number of sectors per cell. The antenna gain patterns for three and six sectors are given in Figure 2 with $10\log a = -15$ dB and $10\log b = -3$ dB.

In our study, all techniques are employed in three-sector cells except the transmit diversity scheme, which is also studied in the six-sector cell case.

4.3. Beamforming techniques

Before we discuss the various beamforming options, we first assume generally that a set of unit-norm transmit weighting vectors $\{\mathbf{w}_j\}_{j=1}^K$ are adopted for the K users' signals at the base station. On denoting $\mathbf{C}_j^i = [\mathbf{c}_j^{i1}, \ldots, \mathbf{c}_j^{iL}]$, $\mathbf{h}_i = [\alpha_{i1}, \ldots, \alpha_{iL}]^T$, and $\mathbf{l}_j^i = \mathbf{C}_j^i \mathbf{h}_i$, a standard space-time RAKE receiver of user i applied in (3) yields

$$\begin{aligned} z_i &= (\mathbf{l}_i^i)^H \mathbf{r}_i \\ &= \sqrt{P_i} b_i \mathbf{w}_i^H \sqrt{G_i} \left(\sum_l \sum_{l'} \alpha_{il'}^* \alpha_{il} (\mathbf{c}_i^{il'})^H \mathbf{c}_i^{il} \mathbf{a}_{il} \right) \\ &\quad + \sum_{k \neq i} \sqrt{P_k} b_k \mathbf{w}_k^H \sqrt{G_i} \left(\sum_l \sum_{l'} \alpha_{il'}^* \alpha_{il} (\mathbf{c}_i^{il'})^H \mathbf{c}_k^{il} \mathbf{a}_{il} \right) \\ &\quad + \sum_{l=1}^{L} \alpha_{il}^* (\mathbf{c}_i^{il})^H \mathbf{n}_i. \end{aligned} \tag{25}$$

With the assumption of

$$\left\langle \mathbf{c}_{k1}^{i,l1}, \mathbf{c}_{k2}^{i,l2} \right\rangle = \begin{cases} 1, & l1 = l2,\ k1 = k2, \\ 0, & l1 = l2,\ k1 \neq k2, \\ \beta, & l1 \neq l2, \end{cases} \tag{26}$$

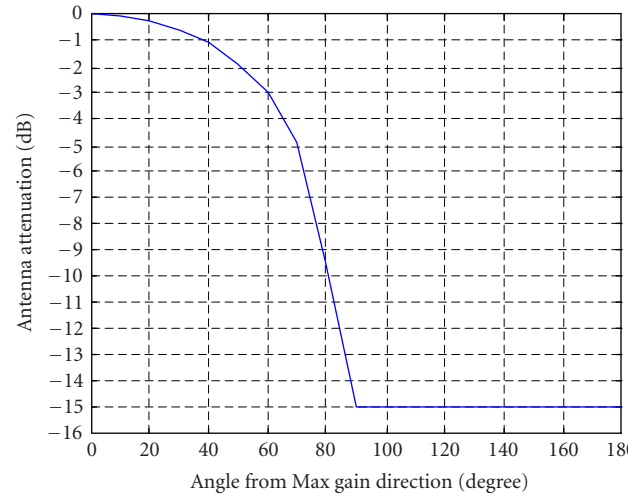

(a)

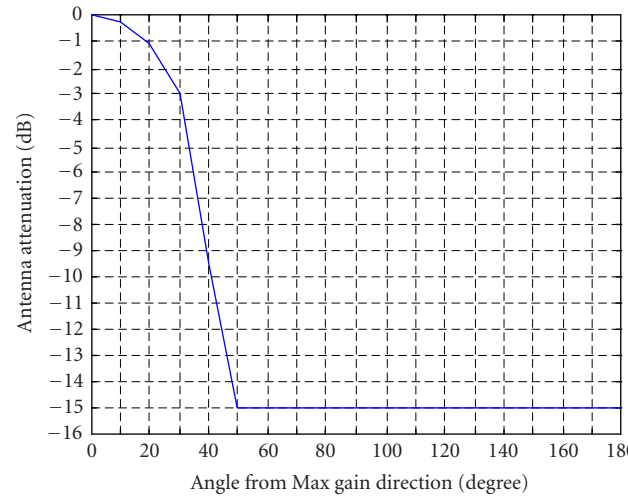

(b)

FIGURE 2: (a) Three-sector antenna radiation pattern. (b) Six-sector antenna radiation pattern.

where β is a random variable defined in (20), and denoting

$$\begin{aligned} \mathbf{R}_i &= G_i \sum_l \sum_{l'} |\alpha_{il}|^2 |\alpha_{il'}|^2 \mathbf{a}_{il} \mathbf{a}_{il'}^H, \\ \mathbf{Q}_i &= \frac{1}{N} G_i \sum_l \sum_{l' \neq l} |\alpha_{il}|^2 |\alpha_{il'}|^2 \mathbf{a}_{il} \mathbf{a}_{il}^H, \end{aligned} \tag{27}$$

the instantaneous SINR for user i is given by

$$\begin{aligned} &\mathrm{SINR}_i \\ &= \frac{P_i \mathbf{w}_i^H \left(\mathbf{R}_i + \mathbf{Q}_i + (1/N) G_i \sum_l \sum_{l' \neq l} |\alpha_{il}|^2 |\alpha_{il'}|^2 \mathbf{a}_{il} \mathbf{a}_{il'}^H \right) \mathbf{w}_i}{\sum_{k \neq i} P_k \mathbf{w}_k^H \mathbf{Q}_i \mathbf{w}_k + \sigma_i^2 \sum_l |\alpha_{il}|^2} \\ &\approx \frac{P_i \mathbf{w}_i^H \mathbf{R}_i \mathbf{w}_i}{\sum_{k \neq i} P_k \mathbf{w}_k^H \mathbf{Q}_i \mathbf{w}_k + \sigma_i^2 \sum_l |\alpha_{il}|^2}. \end{aligned} \tag{28}$$

The power-control formula (10) is exemplified here with

$$\mathbf{D} = \operatorname{diag}(\gamma_1, \ldots, \gamma_K), \tag{29}$$

$$F_{ij} = \begin{cases} 0, & i = j, \\ \dfrac{\mathbf{w}_j^H \mathbf{Q}_i \mathbf{w}_j}{\mathbf{w}_i^H \mathbf{R}_i \mathbf{w}_i}, & i \neq j, \end{cases} \tag{30}$$

$$u_i = \frac{\gamma_i \sigma_i^2 \sum_{l=1}^{L} |\alpha_{il}|^2}{\mathbf{w}_i^H \mathbf{R}_i \mathbf{w}_i}. \tag{31}$$

Since the downlink fading coefficients are not known at the base station, the approximation of Section 2.2 is adopted as follows:

$$\begin{aligned} \overline{\mathbf{R}}_i &= G_i \sum_l \sum_{l'} E\left\{ |\alpha_{il}|^2 |\alpha_{il'}|^2 \right\} \mathbf{a}_{il} \mathbf{a}_{il'}^H, \\ \overline{\mathbf{Q}}_i &= \frac{1}{N} G_i \sum_l \sum_{l' \neq l} E\left\{ |\alpha_{il}|^2 |\alpha_{il'}|^2 \right\} \mathbf{a}_{il} \mathbf{a}_{il}^H, \end{aligned} \tag{32}$$

where the expectation of the small-scale fading coefficients is estimated via time average from uplink data, and the downlink steering vectors are calculated through the estimated DOD, via DOA estimation from uplink data. Based on these matrices, various beamforming schemes are illustrated below. Equations (28), (29), and (31) can be adjusted accordingly.

Beam steering

This is a simple beamforming technique where the transmit antenna array forms a beam in the direction of LOS of the desired user. It corresponds to the following antenna weights:

$$\mathbf{w}_i = \frac{\mathbf{a}^D(\theta_{i,\mathrm{LOS}})}{\left\| \mathbf{a}^D(\theta_{i,\mathrm{LOS}}) \right\|}, \tag{33}$$

where $\theta_{i,\mathrm{LOS}}$ denotes the azimuth angle of the LOS of the ith user with the transmit antenna array.

Maximum SNR

This scheme maximizes the SNR at the ith user. According to (28), it is equivalent to

$$\arg\max_{\mathbf{w}_i} \mathbf{w}_i^H \overline{\mathbf{R}}_i \mathbf{w}_i. \tag{34}$$

It is well known that the solution to (34) is given by the principal eigenvector of the matrix $\overline{\mathbf{R}}_i$.

Maximum SIR/SINR

The maximum SIR scheme transmits as much energy as possible to the desired user while minimizing its interference with other users. Compared with its counterpart on uplink processing, there are two differences for the Max SIR scheme: (1) the interference term is what this signal contributes to the other users, not that seen at the desired mobile; (2) the power levels of transmitted signals are not available at this stage (it is decided at the power control stage), so we cannot conduct maximum SINR as uplink processing. The maximum SIR scheme is formulated as

$$\arg\max_{\mathbf{w}_i} \frac{\mathbf{w}_i^H \overline{\mathbf{R}}_i \mathbf{w}_i}{\mathbf{w}_i^H \overline{\mathbf{T}}_i \mathbf{w}_i} \quad \text{with } \overline{\mathbf{T}}_i = \sum_{k \neq i} \overline{\mathbf{Q}}_k. \tag{35}$$

Such $\mathbf{w}_i$ is given by the generalized principal eigenvector of $[\overline{\mathbf{R}}_i, \overline{\mathbf{T}}_i]$. Compared to Max SNR, this criterion may lead to inadequate power being transmitted to the desired user, or equivalently, may lead to increased transmitted power that results in a type-II outage. Intuitively, there is no benefit in putting too much emphasis on interference minimization at the cost of reduced energy to the desired user, since the noise term cannot be eliminated.

In the packet-switched system, our goal is to maximize the network throughputs with the maximum transmit power, so the power allocation is known in advance. In this case, Max SINR can be exploited as follows:

$$\arg\max_{\mathbf{w}_i} \frac{\mathbf{w}_i^H \overline{\mathbf{R}}_i \mathbf{w}_i}{\mathbf{w}_i^H \overline{\mathbf{T}}_i \mathbf{w}_i} \quad \text{with } \overline{\mathbf{T}}_i = \sum_{k \neq i} \overline{\mathbf{Q}}_k + \frac{K\sigma^2}{P_i} \mathbf{I}, \tag{36}$$

which can be seen as a tradeoff between the Max SNR and Max SIR schemes.

4.4. Joint power control and maximum SINR beamforming

The beamforming approaches given in the last subsection are not the optimum downlink beamforming. While uplink beamforming is a decoupled problem (a chosen weight vector impacts only the desired receiver), in transmit beamforming each transmit weighting affects all the receivers. So downlink beamforming should be done jointly for all users.

The joint power control and beamforming problem was first considered and solved in part in [4, 14], where the uplink joint algorithm is proposed and proved to converge to the optimal solution, and a feasible solution is obtained for the downlink through virtual uplink construction. A complete solution to the joint optimal power control and downlink beamforming is given in [5] through normalization with the noise term (see (28)):

$$\tilde{\mathbf{R}}_i = \frac{\overline{\mathbf{R}}_i}{\sum_l |\alpha_{il}|^2 \sigma_i^2}, \qquad \tilde{\mathbf{Q}}_i = \frac{\overline{\mathbf{Q}}_i}{\sum_l |\alpha_{il}|^2 \sigma_i^2}. \tag{37}$$

The optimization problem is given by

$$\min_{\substack{\mathbf{w}_1, \ldots, \mathbf{w}_K \\ P_1, \ldots, P_K}} \sum_{i=1}^{K} P_i \quad \text{s.t. } \mathrm{SINR}_i \geq \gamma_i, \ \|\mathbf{w}_i\| = 1, \tag{38}$$

with the SINR formula given by

$$\frac{P_i \mathbf{w}_i^H \tilde{\mathbf{R}}_i \mathbf{w}_i}{\sum_{k \neq i} P_k \mathbf{w}_k^H \tilde{\mathbf{Q}}_i \mathbf{w}_k + 1}. \tag{39}$$

The idea is to construct a *virtual uplink problem* with SINR

$$\frac{(P_i)_U \mathbf{w}_i^H \tilde{\mathbf{R}}_i \mathbf{w}_i}{\sum_{k \neq i} (P_k)_U \mathbf{w}_i^H \tilde{\mathbf{Q}}_k \mathbf{w}_i + \|\mathbf{w}_i\|^2}. \tag{40}$$

The following iterations converge to the optimal beamforming vector and power allocation from any initial values for the virtual uplink problem. (The superscript n means the nth iteration.)

Beamforming

For $1 \le i \le K$,

$$\mathbf{w}_i^n = \arg\max_{\mathbf{w}_i} \frac{\mathbf{w}_i^H \tilde{\mathbf{R}}_i \mathbf{w}_i}{\mathbf{w}_i^H \tilde{\mathbf{T}}_i^n \mathbf{w}_i}, \tag{41}$$

where

$$\tilde{\mathbf{T}}_i^n = \sum_{k \ne i} (\mathbf{p}_U^n)_k \tilde{\mathbf{Q}}_k + \mathbf{I}, \tag{42}$$

with $\mathbf{p}_U^n = [(P_1)_U^n, \ldots, (P_K)_U^n]^T$ collecting the power at the nth iteration. This is the decentralized Max SINR scheme whose solution is the principal generalized eigenvector of $[\tilde{\mathbf{R}}_i, \tilde{\mathbf{T}}_i^n]$.

Power control

$$\mathbf{p}_U^{n+1} = \tilde{\mathbf{D}}^n \tilde{\mathbf{F}}_U^n \mathbf{p}_U^n + \tilde{\mathbf{u}}_U^n, \tag{43}$$

where we define

$$\tilde{\mathbf{D}}^n = \operatorname{diag}\left(\gamma_1 / (\mathbf{w}_1^n)^H \tilde{\mathbf{R}}_1 \mathbf{w}_1^n, \ldots, \gamma_K / (\mathbf{w}_K^n)^H \tilde{\mathbf{R}}_K \mathbf{w}_K^n\right), \tag{44}$$

$$(\tilde{\mathbf{F}}_U^n)_{ij} = \begin{cases} 0, & i = j, \\ (\mathbf{w}_i^n)^H \tilde{\mathbf{Q}}_j \mathbf{w}_i^n, & i \ne j, \end{cases} \tag{45}$$

$$(\tilde{\mathbf{u}}_U^n)_i = \frac{\gamma_i \|\mathbf{w}_i^n\|^2}{(\mathbf{w}_i^n)^H \tilde{\mathbf{R}}_i \mathbf{w}_i^n} = (\tilde{\mathbf{D}}^n \mathbf{1}_w^n)_i, \tag{46}$$

where

$$\mathbf{1}_w^n = \left[\left\|\mathbf{w}_1^n\right\|^2, \ldots, \left\|\mathbf{w}_K^n\right\|^2\right]^T = \mathbf{1}. \tag{47}$$

This is the decentralized power control solution (see (11)) when the beamforming vector is fixed. When the above algorithm converges, the optimal virtual uplink power vector is given by

$$\mathbf{p}_U = (\mathbf{I} - \tilde{\mathbf{D}} \tilde{\mathbf{F}}_U)^{-1} \tilde{\mathbf{u}}_U, \tag{48}$$

where $\tilde{\mathbf{D}}$, $\tilde{\mathbf{F}}_U$, and $\tilde{\mathbf{u}}_U$ are converged values of (44), (45), and (46), respectively.

In line with (45) and (46), we define

$$(\tilde{\mathbf{F}}^n)_{ij} = \begin{cases} 0, & i = j, \\ (\mathbf{w}_j^n)^H \tilde{\mathbf{Q}}_i \mathbf{w}_j^n, & i \ne j, \end{cases} \quad \left(\text{i.e., } \tilde{\mathbf{F}}^n = (\tilde{\mathbf{F}}_U^n)^T\right), \tag{49}$$

$$(\tilde{\mathbf{u}}^n)_i = \frac{\gamma_i}{(\mathbf{w}_i^n)^H \tilde{\mathbf{R}}_i \mathbf{w}_i^n} = \tilde{\mathbf{D}}^n \mathbf{1} = (\tilde{\mathbf{u}}_U^n)_i. \tag{50}$$

Then we claim that the optimum downlink power vector is given by

$$\mathbf{p} = (\mathbf{I} - \tilde{\mathbf{D}} \tilde{\mathbf{F}})^{-1} \tilde{\mathbf{u}}, \tag{51}$$

where $\tilde{\mathbf{D}}$, $\tilde{\mathbf{F}}$, and $\tilde{\mathbf{u}}$ are converged values of (44), (49), and (50), respectively. This is because

$$\begin{aligned} \mathbf{1}^T \mathbf{p} &= \mathbf{1}^T (\mathbf{I} - \tilde{\mathbf{D}} \tilde{\mathbf{F}})^{-1} \tilde{\mathbf{D}} \mathbf{1} \\ &= \mathbf{1}^T \tilde{\mathbf{D}} \left(\mathbf{I} - \tilde{\mathbf{D}} (\tilde{\mathbf{F}}_U)^T\right)^{-1} \mathbf{1} \\ &= (\mathbf{p}_U)^T \mathbf{1}, \end{aligned} \tag{52}$$

so the optimality of $\mathbf{p}$ is guaranteed by the optimality of the virtual uplink solution.

5. NUMERICAL RESULTS

In this section we examine the performance of the various downlink transmission techniques discussed above through computer simulation. For circuit-switched systems, power control is carried out and we evaluate and compare the supportable user capacity with certain SINR requirement under some outage limit. For the packet-switched system, we allow each base station to transmit at the maximum power and equally divide the power among the active users. We examine the cumulative distribution function (CDF) of the SINR seen by a typical mobile user for performance comparison since the SINR is directly related to the achievable rate of the user. We also examine the effect of the optimal power assignment scheme of (9).

In our setting, the maximum transmitted power to background noise ratio (out-of-cell interference not included) is set to be 30 dB. The link SINR threshold is 5 dB for circuit-switched systems. The path loss parameter $\eta = 4$, and the standard deviation of the lognormal shadowing is 8 dB. The small-scale fading coefficients are generated through the typical urban (TUx) model used in W-CDMA 3G studies [15]. The users are distributed uniformly within the sector of interest, with the antenna gain pattern given in Figure 2. We assume that for each user there are three multipaths, the angles of which are Gaussian distributed around the direction of LOS, with standard deviation of 10 degrees. The CDMA spreading gain is $N = 64$ for circuit-switched systems and $N = 8$ for packet-switched systems. The number of antennas M in our study is 2, 4, or 8 per sector. We assume each cell has three 120-degree sectors unless otherwise noted. When studying the transmit diversity scheme in the six-sector case, the number of users and antennas per sector is reduced to one half of those in the three-sector scenario.

5.1. Circuit-switched system

Figures 3, 4, and 5 present the performance of the six transmission techniques combined with power control for CDMA downlink circuit-switched systems, namely, transmit diversity, transmit diversity with sectorization, Max SNR beamforming, Max SIR beamforming, beam steering, and joint power control and (Max SINR) beamforming, in the form of supportable user capacity per sector[6] with certain outage. We

[6] Per two sectors for transmit diversity with sectorization.

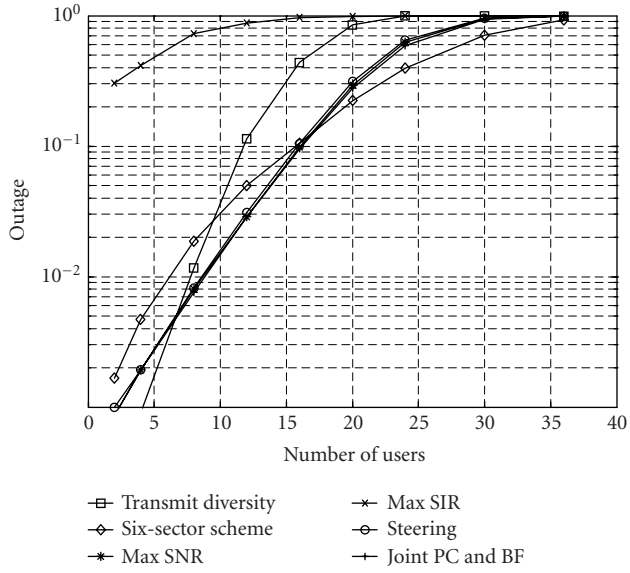

Figure 3: Performance comparison of various transmission techniques with $M = 2$ antennas per sector (6 antennas per cell)—circuit-switched system.

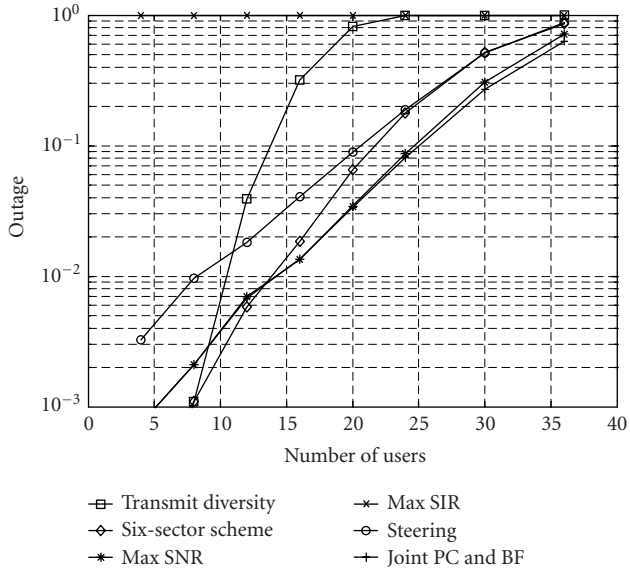

Figure 4: Performance comparison of various transmission techniques with $M = 4$ antennas per sector (12 antennas per cell)—circuit-switched system.

assume no feedback from the mobile. For the sake of comparison, the number of users that can be supported in one cell[7] with 5% outage is given in Table 1, where the results of Max SNR beamforming, and joint power control and beamforming with ideal feedback are also included. From these data, several conclusions can be made for CDMA downlink circuit-switched systems.

[7]Three times the number in Figures 3, 4, and 5.

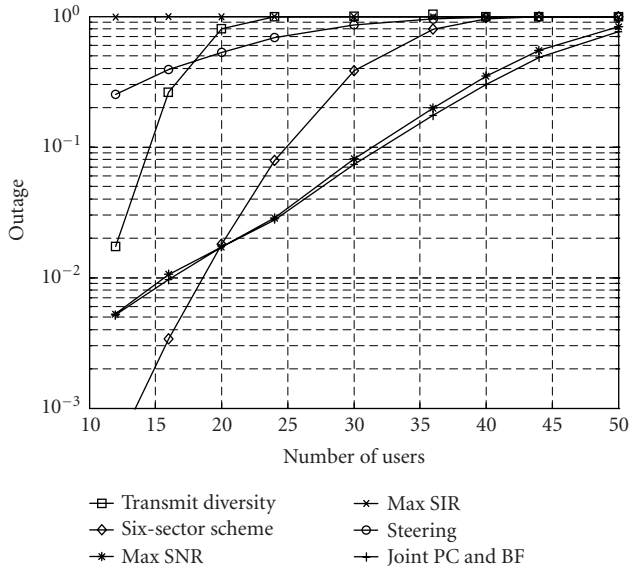

Figure 5: Performance comparison of various transmission techniques with $M = 8$ antennas per sector (24 antennas per cell)—circuit-switched system.

(i) We note that Max SNR beamforming approaches the optimal performance (that of joint power control and Max SINR beamforming) in the outage range of interest, while having much lower complexity, with or without instant downlink CSI.

(ii) For Max SNR beamforming, the gap between that with no feedback and that with feedback increases as the number of antennas increases, but for small numbers of antennas ($M = 2, 4$), the loss due to approximation of channel parameters is insignificant. This means that for small numbers of antennas, Max SNR beamforming is the best choice even without feedback information.

(iii) Max SIR has totally unacceptable performance and thus is omitted in Table 1. As we said before, putting too much emphasis on minimizing the interference to other users will hurt the desired energy; so more power has to be assigned to achieve the SINR threshold, resulting in type-II outage. Another problem with Max SIR is due to the insufficient degrees of freedom the antenna array can offer compared to the number of users for circuit-switched systems.

(iv) Beam steering has good performance only when the number of antenna elements is small ($M = 2$); the gap between beam steering and Max SNR beamforming enlarges as M increases.

(v) For transmit diversity, sectorization significantly improves the performance (6 to 30 more users as M goes from 2 to 8 at 5% outage); but the Max SNR beamforming technique still outperforms the six-sector transmit diversity scheme (6 to 12 more users as M goes from 2 to 8 at 5% outage).

Table 1: Number of users supported in a cell with 5% outage.

Number of antennas per cell	Transmit diversity	Six-sector scheme	Beam steering	Max SNR	Max SNR with feedback	Joint	Joint with feedback
6	30	36	39	42	42	42	42
12	36	57	51	66	72	66	72
24	39	69	12	81	117	84	117

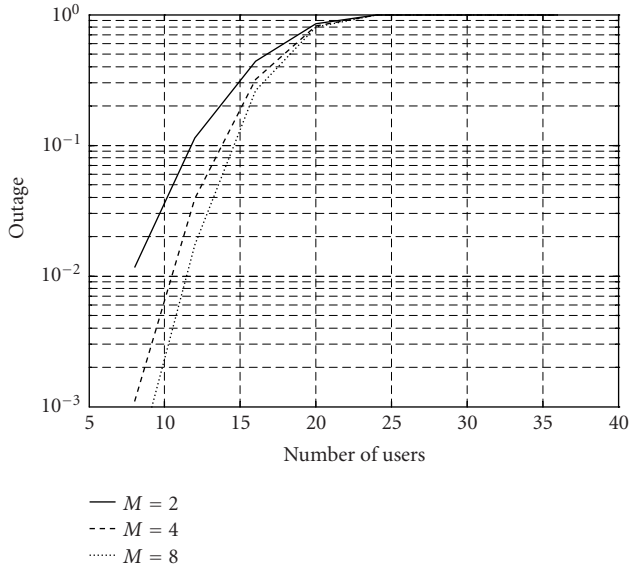

Figure 6: Performance of transmit diversity with 2, 4, and 8 antennas per sector.

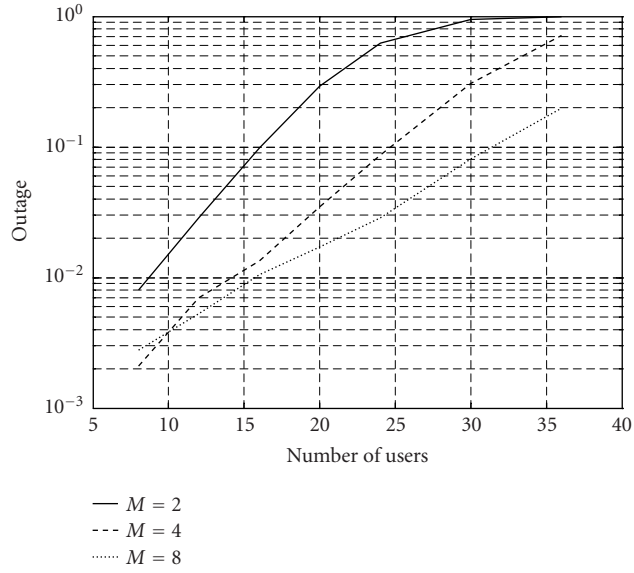

Figure 8: Performance of Max SNR beamforming without feedback with 2, 4, and 8 antennas per sector.

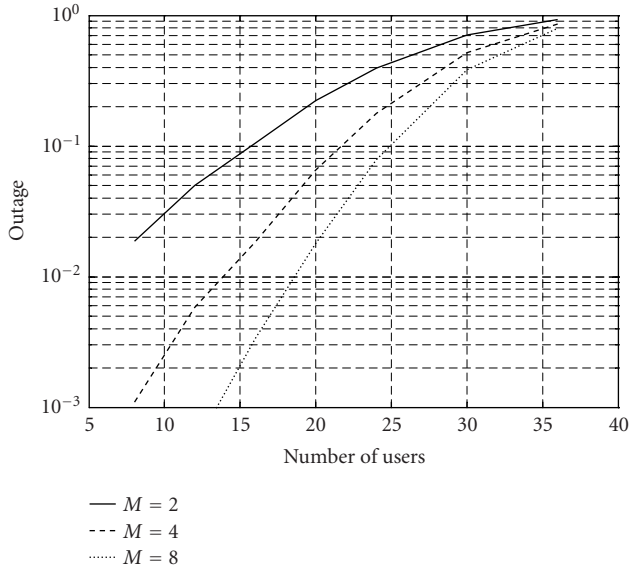

Figure 7: Performance of transmit diversity with sectorization with 2, 4, and 8 antennas per sector.

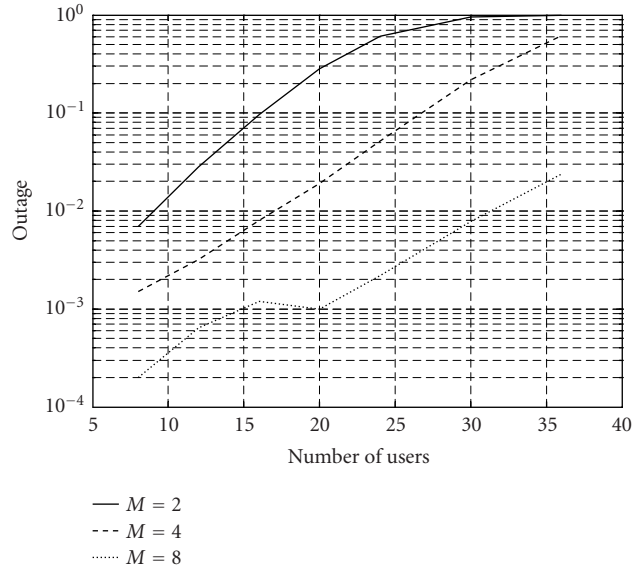

Figure 9: Performance of Max SNR beamforming with feedback with 2, 4, and 8 antennas per sector.

Figures 6, 7, 8, 9, and 10 show the performance of the four transmission techniques as the number of antennas per sector varies from 2, 4 to 8 for circuit-switched systems. Max SIR beamforming is not of interest due to its unacceptable performance. The performance of joint power control and beamforming is similar to that of Max SNR and is omitted here. From these figures, the following conclusions can be drawn.

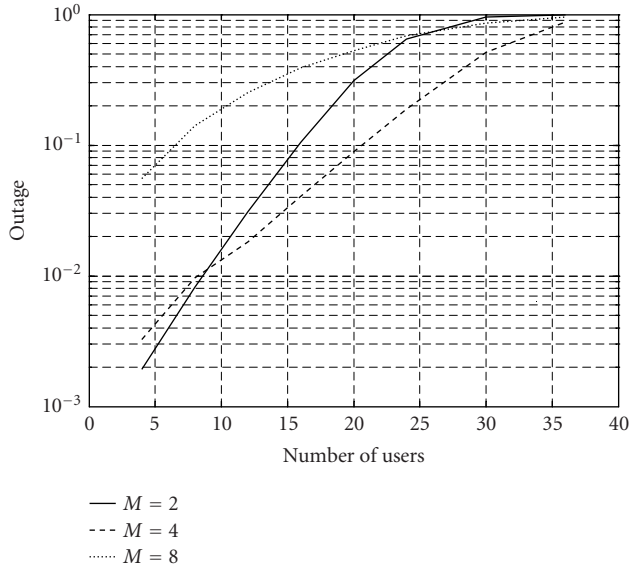

Figure 10: Performance of beam steering with 2, 4, and 8 antennas per sector.

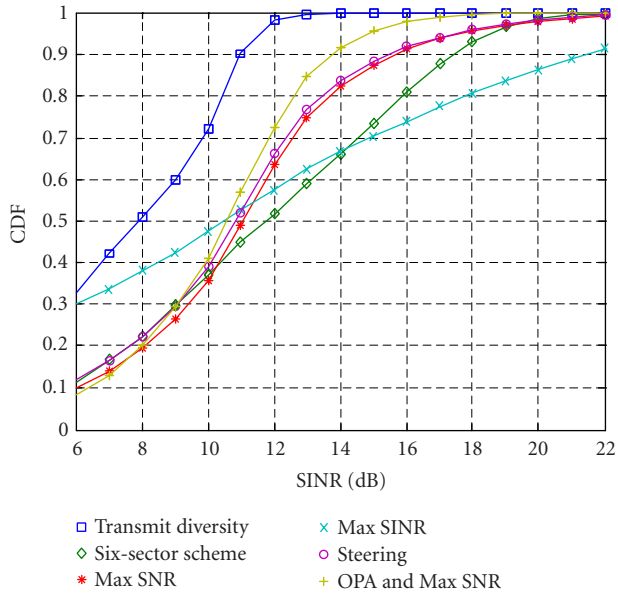

Figure 11: Performance comparison of various transmission techniques with $M = 4$ antennas and $K = 2$ active users—packet-switched system.

(i) For transmit diversity, the gain from exploiting more antennas *diminishes* as the number of antennas increases.

(ii) For Max SNR beamforming, the gain through exploiting, more antenna elements *is restricted* due to imperfect channel knowledge. On the other hand, if we assume ideal feedback, the gain through exploiting more antenna elements *increases* with the number of antennas.

(iii) For beam steering we observe an interesting phenomenon: the performance improves from $M = 2$ to $M = 4$, but deteriorates as M further increases. One possible explanation is that the beam steering scheme forms a beam toward the physical position of the mobile. Due to the angle spread model we use, it actually points in the wrong direction. As more antennas are used, more precise calibration of the LOS actually means greater angle estimation errors. This effect will counteract the benefit of antenna gains with more antennas.

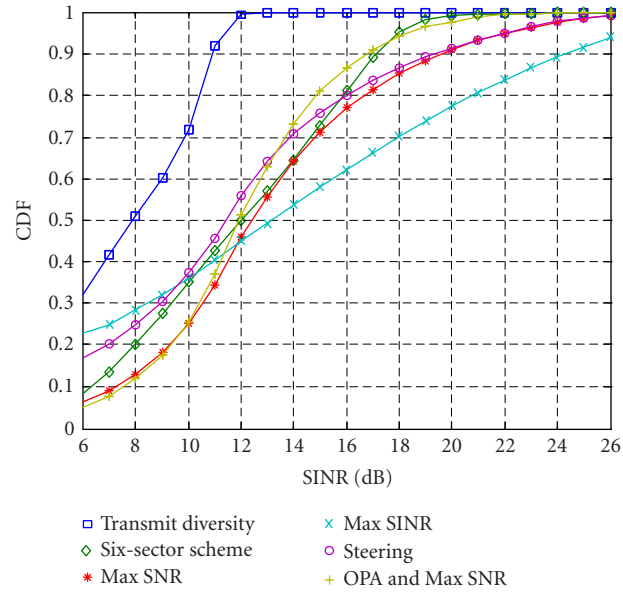

Figure 12: Performance comparison of various transmission techniques with $M = 8$ antennas and $K = 2$ active users—packet-switched system.

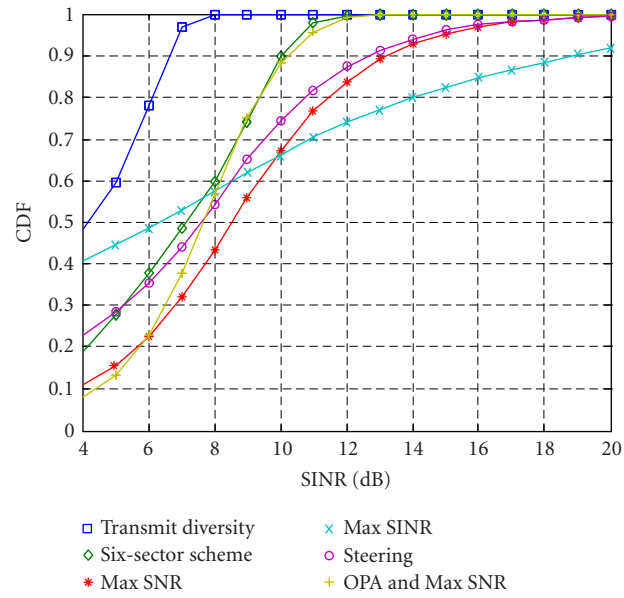

Figure 13: Performance comparison of various transmission techniques with $M = 8$ antennas and $K = 4$ active users—packet-switched system.

5.2. Packet-switched system

As a counterpart to the circuit-switched case, Figures 11, 12, and 13 present the performance of the six transmission

Table 2: Median SINR (50% CDF) of a typical mobile user (dB).

M	K	Transmit diversity	Six-sector scheme	Beam steering	Max SNR	Max SNR (f)	Max SINR	Max SINR (f)	OPA & Max SNR	OPA & Max SNR (f)
4	2	8	11.8	10.8	11	11.1	10.6	10.8	10.6	10.7
8	2	8	12	11.4	12.4	12.7	13.2	13.7	11.9	12.3
8	4	4.2	7.2	7.6	8.5	8.8	6.4	7.2	7.7	8.2

Table 3: Peak SINR (90% CDF) of a typical mobile user (dB).

M	K	Transmit diversity	Six-sector scheme	Beam steering	Max SNR	Max SNR (f)	Max SINR	Max SINR (f)	OPA & Max SNR	OPA & Max SNR (f)
4	2	11	17.5	15.5	15.7	15.7	21.6	21.6	13.8	13.8
8	2	10.8	17.2	19.3	19.5	19.5	24.3	24.6	16.8	17.1
8	4	6.8	10	12.7	13.3	13.4	18.8	19.3	10.3	10.6

techniques for packet-switched systems. We perform equal power assignment unless otherwise noted. The optimal power allocation combined with Max SNR serves as a performance baseline. In contrast with circuit-switched systems, we can implement the maximum SINR scheme here as we have knowledge of the power allocation. For the sake of comparison, the median (50% CDF) and peak (90% CDF) SINR values seen by a typical user are given in Tables 2 and 3, respectively. Note that for the $M = 8$ and $K = 4$ case, the simultaneously transmitted users are doubled. One should consider this when translating SINR to achievable rates and network throughput. "(f)" in the tables designates results with feedback channel parameter information. From these data, several conclusions can be drawn for CDMA downlink packet-switched systems.

(i) OPA has no benefit in packet-switched systems. We see from Figures 11, 12, and 13 that, the Max SNR with OPA, compared with Max SNR with equal power allocation, favors low-rate (low SINR) users but harms high-rate (high SINR) users. As we discussed in Section 3, optimal power allocation is like a socialist scheme that seeks absolute fairness. It cannot achieve the highest throughput and, without being jointly considered with the link and network schedules, cannot guarantee fairness either. A similar phenomenon can be observed for the Max SINR scheme and is omitted here.

(ii) Contrary to the circuit-switched case, Max SINR beamforming has the best performance in terms of peak rate; it is also good at median rate with small numbers of users, while comparable with others when there are more users.

(iii) Max SNR beamforming is almost the best in terms of median rate; it is also good in terms of peak rate performance.

(iv) Beam steering is almost as good as Max SNR in terms of peak rate performance, while a little worse (1 dB) in terms of median rate performance.

(v) For transmit diversity, sectorization significantly improves the performance (4–7 dB).

(vi) The Max SNR beamforming technique outperforms the six-sector transmit diversity scheme for $M = 8$ (1 dB in median and 2–3 dB in peak); for $M = 4$, six-sector transmit diversity is better.

Figures 14, 15, and 16 compare the performances of Maximum SINR beamforming with and without feedback. We find that feedback does not help much. Similar results hold for other beamforming techniques in packet-switched systems and are omitted here.

6. CONCLUSIONS

In this paper, we have seen that traffic type impacts the algorithm choice in CDMA cellular downlink transmission with antenna arrays in multipath fading channels. For circuit-switched downlink CDMA systems, the Max SNR beamforming scheme is the best choice (accommodating 12 to 42 more users than transmit diversity). For packet-switched systems, Max SINR beamforming has the best performance in terms of peak rate (10–14 dB more than transmit diversity); Max SNR beamforming is almost the best in terms of median rate (3–4 dB more than transmit diversity), but beam steering and transmit diversity with sectorization are also good choices. Optimum power control/allocation schemes have been shown to be either too complex or infeasible in practice. In circuit-switched systems, the gap between the performance with no feedback channel information and that with feedback increases as the number of antennas increases, but for small numbers of antennas, the loss due to approximation of channel parameters is insignificant. On the other hand, feedback channel information does not help much for beamforming techniques in packet-switched systems. We also see that sectorization greatly improves the system performance, both for the circuit-switched and for the packet-switched systems.

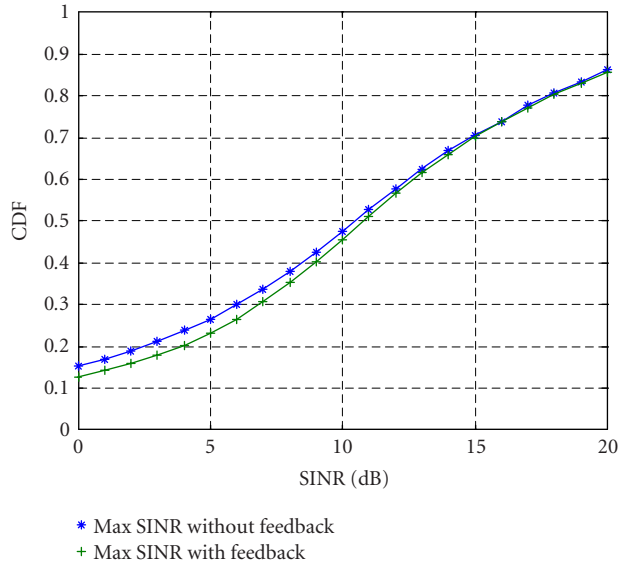

FIGURE 14: Performance of Max SINR beamforming with $M = 4$ antennas and $K = 2$ active users, with and without feedback channel information.

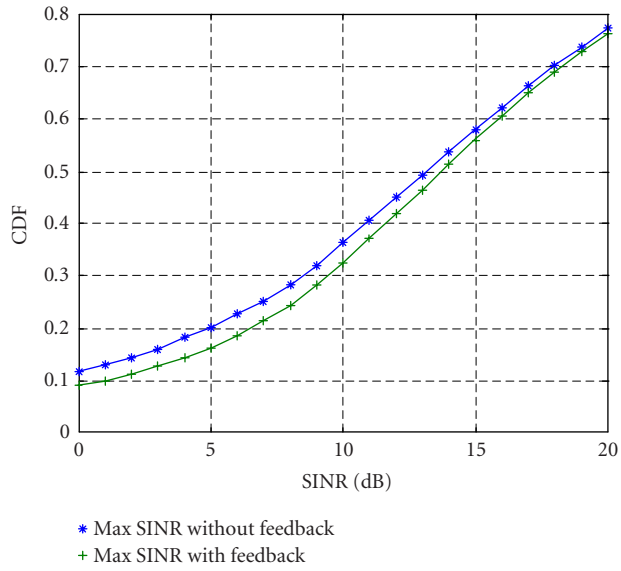

FIGURE 15: Performance of Max SINR beamforming with $M = 8$ antennas and $K = 2$ active users, with and without feedback channel information.

The following issues deserve further study in this context. In this paper, we have assumed the perfect knowledge of the DOD when calculating the downlink spatial covariance matrix. The issue of parameter estimation errors in covariance matrix calculation is of interest. Other interesting topics include joint consideration of link and network schedules with transmission techniques in packet-switched systems, and array processing techniques to combat the large-scale fading exploiting widely separated antennas (macrodiversity).

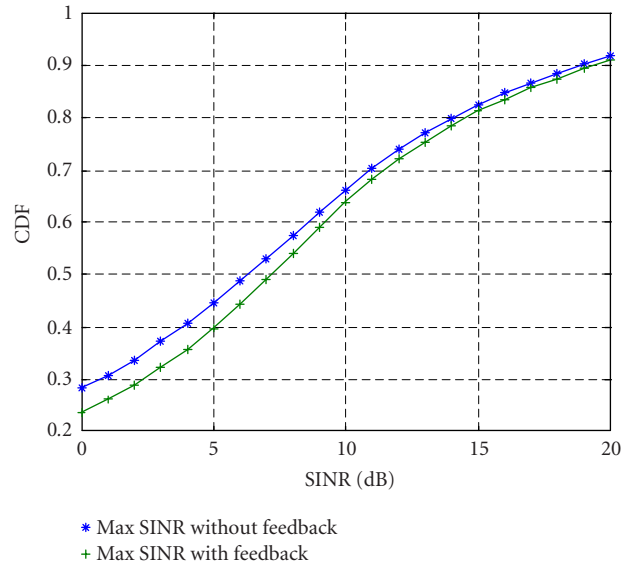

FIGURE 16: Performance of Max SINR beamforming with $M = 8$ antennas and $K = 4$ active users, with and without feedback channel information.

ACKNOWLEDGMENTS

The authors would like to thank Doctors Dmitry Chizhik, Constantinos Papadias, Jerry Foschini, Mike Gans, Howard Huang, Jack Salz, Reinaldo Valenzuela, and all other members of the Wireless Communications Research Department of Bell Labs, Lucent Technologies, for helpful discussions. Part of this work was done while Huaiyu Dai was a summer intern there. This research was supported in part by Bell Labs, Lucent Technologies, in part by the National Science Foundation under Grant CCR 99-80590, and in part by the New Jersey Center for the Wireless Telecommunications.

REFERENCES

[1] J. H. Winters, J. Salz, and R. D. Gitlin, "The impact of antenna diversity on the capacity of wireless communication systems," *IEEE Trans. Communications*, vol. 42, no. 2,3,4, pp. 1740–1751, 1994.

[2] B. D. Van Veen and K. M. Buckley, "Beamforming: a versatile approach to spatial filtering," *IEEE Signal Processing Magazine*, vol. 5, no. 2, pp. 4–24, 1988.

[3] T. S. Rappaport, *Wireless Communications: Principles and Practice*, Prentice-Hall PTR, Upper Saddle River, NJ, USA, 2nd edition, 2002.

[4] F. Rashid-Farrokhi, L. Tassiulas, and K. J. R. Liu, "Joint optimal power control and beamforming in wireless networks using antenna arrays," *IEEE Trans. Communications*, vol. 46, no. 10, pp. 1313–1324, 1998.

[5] E. Visotsky and U. Madhow, "Optimum beamforming using transmit antenna arrays," in *Proc. IEEE Vehicular Technology Conference (VTC '99)*, vol. 1, pp. 851–856, Houston, Tex, USA, May 1999.

[6] S. V. Hanly and D. Tse, "Power control and capacity of spread-spectrum wireless networks," *Automatica*, vol. 35, no. 12, pp. 1987–2012, 1999.

[7] B. Hochwald, T. L. Marzetta, and C. B. Papadias, "A transmitter diversity scheme for wideband CDMA systems based

on space-time spreading," *IEEE Journal on Selected Areas in Communications*, vol. 19, no. 1, pp. 48–60, 2001.
[8] A. J. Paulraj and C. B. Papadias, "Space-time processing for wireless communications," *IEEE Signal Processing Magazine*, vol. 14, no. 6, pp. 49–83, 1997.
[9] G. G. Raleigh, S. N. Diggavi, V. K. Jones, and A. Paulraj, "A blind adaptive transmit antenna algorithm for wireless communication," in *Proc. IEEE International Conference on Communications (ICC '95)*, vol. 3, pp. 1494–1499, Seattle, Wash, USA, June 1995.
[10] B. M. Hochwald and T. L. Maretta, "Adapting a downlink array from uplink measurements," *IEEE Trans. Signal Processing*, vol. 49, no. 3, pp. 642–653, 2001.
[11] T. Aste, P. Forster, L. Fety, and S. Mayrargue, "Downlink beamforming avoiding DOA estimation for cellular mobile communications," in *Proc. 1989 IEEE International Conference on Acoustics, Speech, and Signal Processing (ICASSP '98)*, vol. 6, pp. 3313–3316, Seattle, Wash, USA, May 1998.
[12] W. Yang and G. Xu, "Optimal downlink power assignment for smart antenna systems," in *Proc. 1998 IEEE International Conference on Acoustics, Speech, and Signal Processing (ICASSP '98)*, pp. 3337–3340, Seattle, Wash, USA, May 1998.
[13] H. Minc, *Nonnegative Matrices*, Wiley, New York, NY, USA, 1988.
[14] F. Rashid-Farrokhi, K. J. R. Liu, and L. Tassiulas, "Transmit beamforming and power control for cellular wireless systems," *IEEE Journal on Selected Areas in Communications*, vol. 16, no. 8, pp. 1437–1450, 1998.
[15] V. K. Garg, *IS-95 CDMA and cdma2000: Cellular/PCS Systems Implementation*, Prentice-Hall, Upper Saddle River, NJ, USA, 2000.

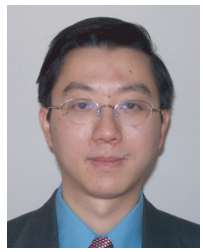

Huaiyu Dai received the B.E. and M.S. degrees in electrical engineering from Tsinghua University, Beijing, China, in 1996 and 1998, respectively, and the Ph.D. degree in electrical engineering from Princeton University, Princeton, NJ, in 2002. He worked at Bell Labs, Lucent Technologies, Holmdel, NJ, during the summer of 2000, and at AT&T Labs – Research, Middletown, NJ, during the summer of 2001. Currently he is an Assistant Professor of electrical and computer engineering at NC State University. His research interests are in the general areas of communication systems and networks, advanced signal processing for digital communications, and communication theory and information theory. He has worked in the areas of digital communication system design, speech coding and enhancement, and DSL transmission. His current research focuses on space-time communications and signal processing, the turbo principle and its applications, multiuser detection, and the information-theoretic aspects of multiuser communications and networks.

Laurence Mailaender received his Ph.D. in electrical engineering from the University of California at Santa Barbara in 1996. His doctoral research concerned near-optimal multiuser detection of CDMA signals with joint amplitude and delay estimation. In 1996, Dr. Mailaender joined Bell Labs, Lucent Technologies, in the Wireless Communications Research Department. During 2000–2001 he led a team developing advanced receiver algorithms for MIMO systems on delay-dispersive channels. This led to ASIC implementation and over-the-air testing of the algorithms, including MIMO equalization. His current work is focused on MIMO systems with advanced equalization.

H. Vincent Poor received the Ph.D. degree in EECS from Princeton University in 1977. From 1977 until 1990, he was with the faculty of the University of Illinois at Urbana-Champaign. Since 1990 he has been with the faculty of Princeton, where he is the George Van Ness Lothrop Professor in Engineering. Dr. Poor's research interests are in the areas of wireless networks, advanced signal processing, and related fields. Among his publications in these areas is the recent book *Wireless Communication Systems: Advanced Techniques for Signal Reception* (2004). Dr. Poor is a member of the US National Academy of Engineering, and is a Fellow of the IEEE, the Institute of Mathematical Statistics, the Optical Society of America, and other organizations. In 1990, he served as President of the IEEE Information Theory Society, and in 1991–1992 he was a Member of the IEEE Board of Directors. Among his recent honors are the IEEE Graduate Teaching Award (2001), the Joint Paper Award of the IEEE Communications and Information Theory Societies (2001), the NSF Director's Award for Distinguished Teaching Scholars (2002), a Guggenheim Fellowship (2002–2003), and the Distinguished Teacher Award of the Princeton School of Engineering and Applied Science (2003).